

Overly persistent circulation in climate models contributes to overestimated frequency and duration of heat waves and cold spells

Eva Plavcová¹ · Jan Kyselý^{1,2}

Received: 23 December 2014 / Accepted: 29 June 2015 / Published online: 23 July 2015
© Springer-Verlag Berlin Heidelberg 2015

Abstract The study examines links of summer heat waves and winter cold spells in Central Europe to atmospheric circulation and specifically its persistence in an ensemble of regional climate models (RCMs). We analyse 13 RCMs driven by the ERA-40 reanalysis and compare them against observations over reference period 1971–2000. Using objective classification of circulation types and an efficiency coefficient with a block resampling test, we identify circulation types significantly conducive to heat waves and cold spells. We show that the RCMs have a stronger tendency to group together days with very high or low temperature and tend to simulate too many heat waves and cold spells, especially those lasting 5 days and more. Circulation types conducive to heat waves in summer are characterized by anticyclonic, southerly and easterly flow, with increasing importance of warm advection during heat waves. Winter cold spells are typically associated with easterly and anticyclonic flow, and the onset of cold spells tends to be linked to northerly and cyclonic flow with cold advection. The RCMs are generally able to reproduce the links between circulation and heat waves or cold spells, including the radiation-to-advection effect for heat waves and the opposite advection-to-radiation effect for cold spells. They capture relatively well also changes of mean temperature anomalies during sequences of given circulation types, namely the tendency towards temperature increase (decrease) during those types conducive to heat waves (cold spells). Since mean lengths of all

circulation supertypes are overestimated in the RCMs, we conclude that the overly persistent circulation in climate models contributes to the overestimated frequency of long heat waves and cold spells. As these biases are rather general among the examined RCMs and similar drawbacks are likely to be manifested in climate model simulations for the twenty-first century, the results also suggest that climate change scenarios for spells of days with high or low temperatures should be interpreted with a view to the models' limitations in simulating the recent climate.

Keywords Heat wave · Cold spell · Atmospheric circulation · Persistence · Regional climate models · Central Europe

1 Introduction

Heat waves (HWs) and cold spells (CSPs) are atmospheric phenomena with potentially disastrous effects on human society and the natural environment in mid-latitudes. Their impacts include excess human and animal mortality, wild-fires, decreased agricultural production, power outages, lack of cooling energy supply, and overall economic losses (e.g. Beniston 2004; De Bono et al. 2004; Ciais et al. 2005; Vavrus et al. 2006; Robine et al. 2008; Barriopedro et al. 2011; Kyselý et al. 2011). Because society will likely be strongly affected if such events increase in frequency, intensity and persistence in future, it is important to study characteristics of HWs and CSPs as simulated by climate models, and especially to validate how they are reproduced in simulations for the recent climate. Possible drawbacks of climate models in capturing dynamic causes of extreme temperature events would reduce confidence in the simulation of HWs and CSPs in a future climate.

✉ Eva Plavcová
plavcova@ufa.cas.cz

¹ Institute of Atmospheric Physics AS CR, Boční II 1401, 141 31 Prague, Czech Republic

² Faculty of Environmental Sciences, Czech University of Life Sciences, Prague, Czech Republic

Many studies have reported increases in the number and length of HWs in the observed data (Alexander et al. 2006; Moberg et al. 2006; Della-Marta et al. 2007; Kyselý 2010) as well as in scenarios of climate change (Meehl and Tebaldi 2004; Ballester et al. 2010). Using the PRUDENCE regional climate models (RCMs), Beniston et al. (2007) found that the same number of hot days in Southern Europe for the recent climate may become typical for Central Europe by the end of the twenty-first century. Based on RCMs from the more recent ENSEMBLES project, Fischer and Schär (2010) demonstrated that in comparison to present conditions the frequency of Central European hot days is projected to increase by a factor of 10 in the 2071–2100 period.

Although the number of CSPs has declined significantly since the 1950s (Hartmann et al. 2013) and these events are expected to be less severe in the future climate due to an increase of global temperature (Kirtman et al. 2013), this might be altered through modulation of a large-scale flow over Europe related to a decline in the extent of Arctic sea ice (Francis and Vavrus 2012; Tang et al. 2013) and/or changes in solar activity (Huth et al. 2008; Lockwood et al. 2010). These suggest that severe CSPs will probably occur despite global warming conditions, as showed by Kodra et al. (2011).

In mid-latitudes, the large-scale atmospheric circulation is one of the key determinants of climate and its variability. In a previous study (Plavcová and Kyselý 2012), we examined the capability of ENSEMBLES RCMs to simulate atmospheric circulation and relationships between circulation and daily surface air temperatures over Central Europe within individual seasons. In the present study, we extend that analysis towards links between atmospheric circulation and spells of high and low temperature extremes. Extreme temperatures (both high and low) are triggered by an interruption of prevailing zonal westerly flow and a development of blocking conditions (Sillmann et al. 2011; Schneidereit et al. 2012). Occurrence of long and severe HWs or CSPs is primarily related to persistent or recurring circulation patterns which influence an area over prolonged time periods and support positive or negative anomalies of surface air temperature (Kyselý 2008). It is therefore useful to detect which circulation patterns are conducive to extreme temperatures over Europe (Domonkos et al. 2003; Cassou et al. 2005; Kyselý 2007) and to study whether climate models are able to reproduce the links between circulation and development of HWs or CSPs. Another focus of this study is to examine how persistence of atmospheric patterns is simulated and whether its biases may affect reproduction of the lengths of HWs and CSPs.

The aims of this paper are to analyse how RCMs capture the frequency and duration of extreme temperature periods in Central Europe, as well as whether the biases are

linked to simulated atmospheric circulation and its persistence. Atmospheric circulation is represented by a widely used classification into 27 circulation types based on circulation indices derived from daily mean sea level pressure (Jenkinson and Collison 1977; Jones et al. 1993; Demuzere et al. 2009). Although this methodology does not take into account other processes essential in the evolution of HWs and CSPs, such as the role of persistent pressure and temperature anomalies at other vertical levels (Miralles et al. 2014) or land–atmosphere coupling (Jaeger and Seneviratne 2011), it is a useful method for studying the basic processes related to atmospheric dynamics. We analyse simulations of 13 RCMs driven by the ERA-40 reanalysis over the 30-year period 1971–2000 while focusing on HWs in summer and CSPs in winter.

The paper is structured as follows: The data and methods are described in Sect. 2. Statistics of observed and simulated HWs and CSPs are shown in Sect. 3.1. Section 3.2 provides an analysis of circulation types conducive to HWs and CSPs. Links between persistence of circulation types and temperature anomalies are analysed in Sect. 3.3. Finally, we examine differences in simulated and observed persistence of circulation types in Sect. 3.4. Discussion and conclusions follow in Sects. 4 and 5.

2 Data and methods

2.1 Data

An ensemble of 13 RCMs from the ENSEMBLES project (van der Linden and Mitchell 2009) is examined. The models have spatial resolution of about 25 km (0.22°). We analyse simulations driven by reanalysis (ERA-40; spatial resolution of 2.5° ; Uppala et al. 2005), which is regarded as a perfect boundary condition and avoids biases caused by potentially biased global climate model boundary conditions. The RCMs are listed and references to further details are given in Table 1.

Daily maximum and minimum temperatures and daily mean sea level pressure data are examined over the 30-year period of 1971–2000. As reference data, we use the gridded E-OBS data set (version 7, Haylock et al. 2008) for temperature and the ERA-40 reanalysis for pressure data. The E-OBS data set had been constructed within the ENSEMBLES project specifically for the validation of RCMs and uses the same grid as do most of the RCMs. To characterize mean cloud cover conditions before and during HWs or CSPs, we use total cloud amount data from the Milešovka meteorological station (837 m a.s.l.) situated on a free-standing mountain close to the middle of the examined domain (50.6°N and 13.9°E).

Table 1 Summary of the examined ENSEMBLES regional climate models

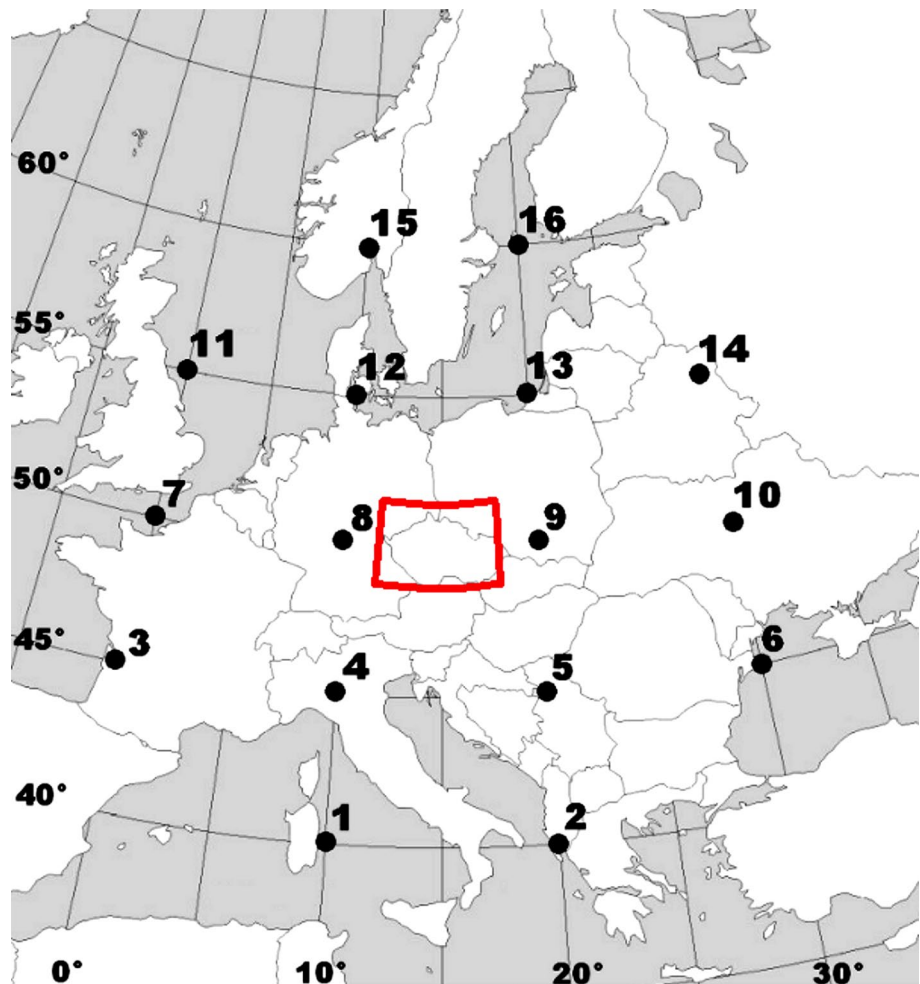
Institute	Model	Reference
C4I	RCA3	Kjellström et al. (2005)
CHMI	Aladin	Farda et al. (2010)
CNRM	Aladin	Radu et al. (2008)
DMI	HIRHAM	Christensen et al. (1996)
EC	GEMLAM	
ETHZ	CLM	Böhm et al. (2006)
HC	HadRM3Q0	Collins et al. (2006)
ICTP	RegCM	Giorgi et al. (2004)
KNMI	RACMO	van Meijgaard et al. (2008)
METNO	HIRHAM	Haugen and Haakenstad (2006)
MPI	REMO	Jacob (2001)
SMHI	RCA	Samuelsson et al. (2011)
OURANOS	CRCM	Plummer et al. (2006)

2.2 Methods

2.2.1 Definitions of heat waves and cold spells

Daily temperature series were first averaged over a Central European region defined as the area from 48.5°N to 51.5°N and from 12°E to 18°E (shown in Fig. 1). Averaging over the domain (237 grid points in most RCMs) assures that only events with larger-scale spatial extent and impacts are selected. Anomalies of daily maximum (TX) and minimum (TN) temperatures from their mean annual cycles (smoothed by 7-day running means) were then computed. Hot (cold) days were defined as days with TX (TN) above (below) the 90 % (10 %) quantile of their empirical distributions in summer (winter). Summer was considered as June–August (JJA) and winter as December–February (DJF). The quantiles were calculated for the observed data and each individual

Fig. 1 Region under study (area between 48.5°N and 51.5°N, and 12°E and 18°E), across which the temperature data were averaged and 16 grid points used to construct the airflow indices



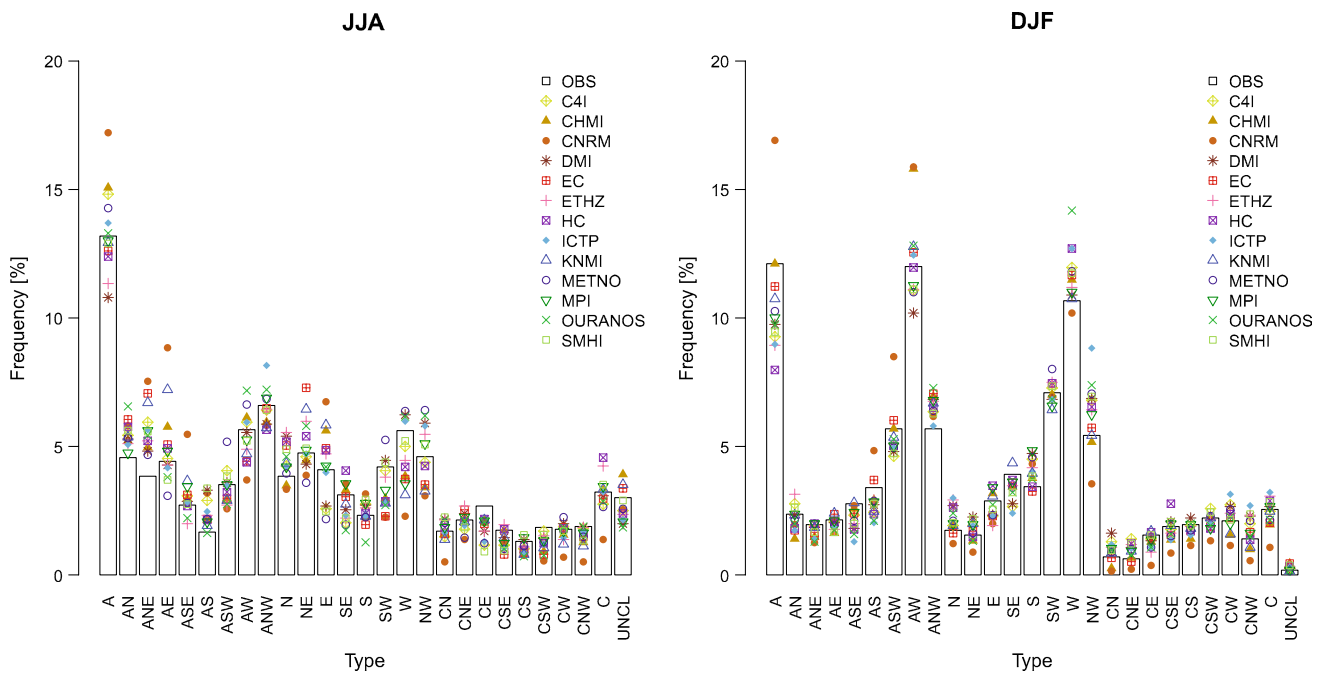


Fig. 2 Summer (JJA) and winter (DJF) frequencies of circulation types in the observed data (ERA-40, bars) and in RCM simulations (points) during 1971–2000

RCM separately, as the study is focused not on temperature bias in the RCMs themselves but rather on the characteristics of spells of hot and cold days. An analogous approach has been widely used in studies dealing with the evaluation of extreme temperature events in climate models (e.g. Peings et al. 2013; Vautard et al. 2013).

Heat waves (HWs) are defined as periods of at least three consecutive hot days in JJA, while CSPs consist of at least three consecutive cold days in DJF. All subsequent hot (cold) days are attached to a HW (CSP) as long as there is no break longer than 1 day with TX below the threshold (TN above the threshold). This is done to avoid having multiple short HWs or CSPs in cases when they are separated only by a single day not meeting the criterion for a hot or cold day (which may typically be associated with passage of a weak cold front in summer or warm or occluded front in winter) and which does not change the overall weather pattern on synoptic time scales. An advantage of this definition is that it is relative, based on deviations from the mean annual temperature cycle, and no seasonal- or location-specific temperature thresholds are needed. This allows for a more straightforward analysis of links to atmospheric circulation, as well as for application of the definition in studies for other regions.

2.2.2 Characteristics of atmospheric circulation

Atmospheric circulation is represented by 27 circulation types defined using three circulation indices [flow

direction, strength (STR), and vorticity (VORT); Jenkinson and Collison 1977; Jones et al. 1993]. The indices are derived from daily gridded mean sea level pressure data at the 16 grid points shown in Fig. 1 using equations provided in Plavcová and Kyselý (2012). To avoid a high percentage of unclassified days (particularly in summer), we slightly modified the classification of Jones et al. (1993) which had been set up originally for the area of the British Isles (where STR and VORT tend to reach higher values; cf. Blenkinsop et al. 2009 vs. Plavcová and Kyselý 2012). In our classification, if $|VORT| \geq 4 * STR$, then strongly cyclonic ($VORT > 0$; C) and anticyclonic ($VORT < 0$; A) types are defined. If $|VORT| < STR$, there are eight directional types (divided into eight quadrants: N, NE, E, SE, S, SW, W, and NW). Sixteen hybrid types (combinations of directional and cyclonic/anticyclonic types, i.e. CN, AN, CNE, ANE, etc.) are characterized by $|VORT| \geq STR$ and $|VORT| < 4 * STR$. If $|VORT| < 3$ and $STR < 3$, then the days are considered unclassified (UNCL). More details are given in Plavcová et al. (2014). An advantage afforded by these predefined circulation types based on simple flow characteristics lies in its ability to visualize basic features of individual circulation patterns without plotting maps of the classified variables for each type.

Westerly flow predominates over Central Europe in the observed data, especially in winter, but, among individual types, the strongly anticyclonic type occurs with the highest frequency in both seasons (Fig. 2). The ability of a set

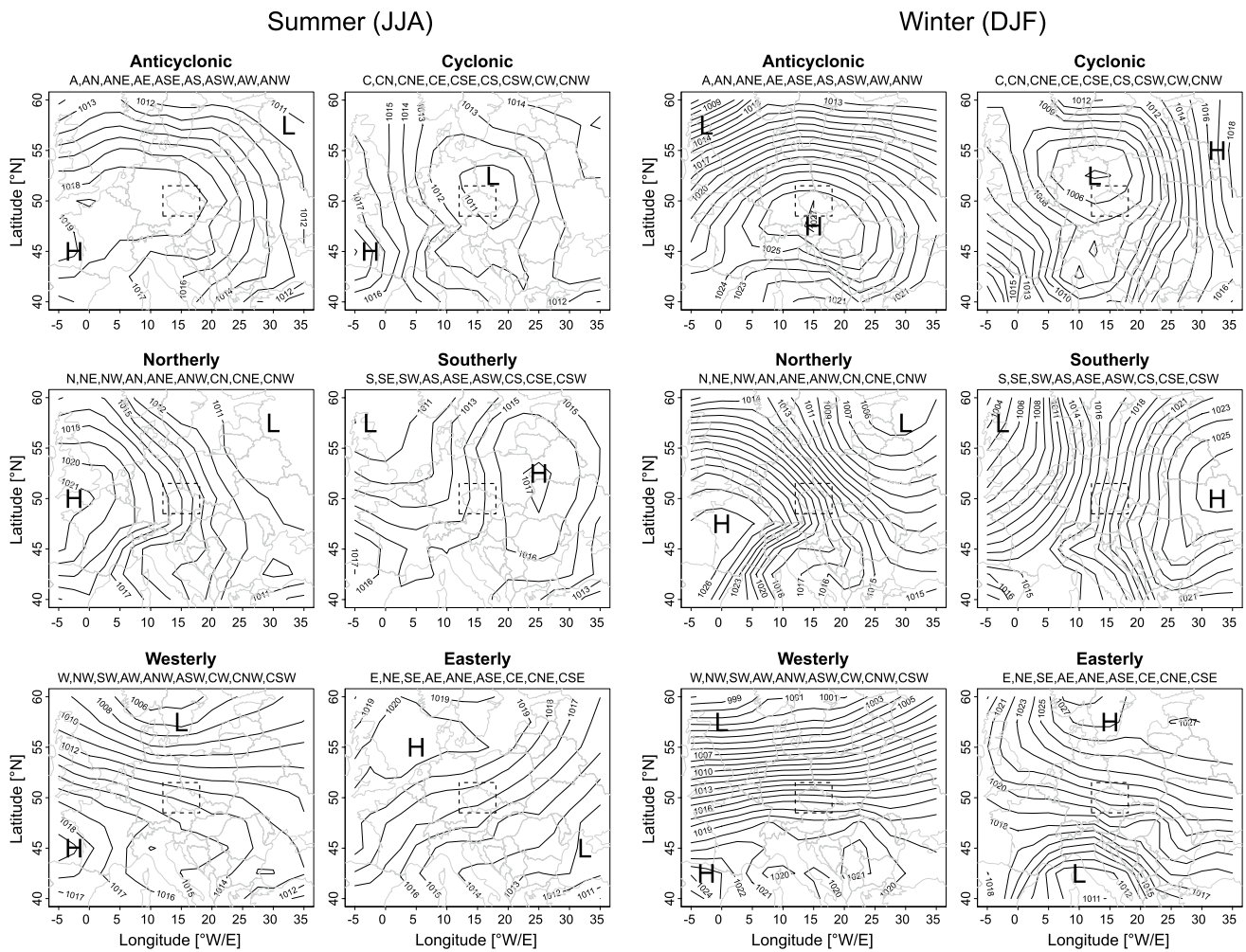


Fig. 3 Mean sea level pressure fields averaged over days within given circulation supertypes in summer and winter. *H/L* marks areas of high/low pressure; the *dashed line* shows the area under study

(Central Europe). Circulation types included in a given supertype are listed at the *upper margin* of each plot. Data from the ERA-40 reanalysis over 1971–2000 were used

of the ENSEMBLES RCMs to reproduce atmospheric circulation over Central Europe as represented by flow direction, strength, and vorticity is discussed in detail in our previous work (Plavcová and Kyselý 2012). The main findings remain unchanged for the set of RCMs used in the present study: The RCMs are generally able to reproduce qualitatively the observed distributions of the circulation types as well as their seasonal changes, although quantitatively they have biases (Fig. 2). Among the deficiencies common to most of the RCMs are overestimation of westerly flow and underestimation of strongly anticyclonic types in winter, as well as overestimation of northerly flow in summer.

Since frequencies of some circulation types are low, as shown in Fig. 2, we grouped the types into ‘supertypes’ (cf. Kyselý and Huth 2006) in order to obtain more robust results in analysing the persistence of atmospheric circulation. We defined six supertypes: northerly, southerly, easterly, westerly, cyclonic, and anticyclonic. Each supertype is

comprised of 9 circulation types with a given flow characteristic (for example, the northerly supertype is comprised of N, NE, NW, CN, CNE, CNW, AN, ANE, and ANW types, while the cyclonic supertype is comprised of C, CN, CNE, CE, CSE, CS, CSW, CW, and CNW types). The types within each supertype are listed in Fig. 3. Observed frequencies of the circulation types and supertypes are reported in Table 2, and mean pressure patterns of the supertypes are shown in Fig. 3.

Statistical significance of differences between observed and modelled mean lengths of day sequences within given circulation supertypes were tested using the Wilcoxon–Mann–Whitney test.

2.2.3 Efficiency coefficient

Types conducive to HWs are evaluated in terms of an efficiency coefficient calculated as the ratio of the relative

frequency of a given circulation type before or during HWs to its long-term mean seasonal frequency (Kyselý 2007). We analyse the efficiency coefficient (i) for 3 days ($D - 3$ to $D - 1$) before the beginning of a HW, (ii) for the first 3 days of a HW ($D + 0$ to $D + 2$), and (iii) for all days in a HW ($D + 0$ to $D + x$, where x represents the length of an individual HW). CSPs were treated in the same way.

Statistical significance of the efficiency coefficient was tested using the block resampling method: the same number of 3-day sequences (for i and ii) of circulation types

as the frequency of HWs (CSPs) was sampled 10,000 times in JJA (DJF) to estimate the distribution of the seasonal efficiency coefficient for individual circulation types. The efficiency coefficient is statistically significant if it is higher (lower) than the 95 % (5 %) quantile of the estimated seasonal distribution. For (iii), it is tested analogously but the lengths of the blocks are taken as the lengths of the spells. Values of the coefficient significantly higher than 1 define types considered as conducive to HWs or CSPs.

Table 2 Observed summer and winter mean relative frequencies of circulation types and supertypes during 1971–2000, and efficiency coefficients for 3 days before the beginning of HWs or CSPs, the first 3 days of HWs or CSPs, and all days in HWs or CSPs

Type/super-type	Mean JJA freq. (%)	Days before HWs ($D - 3$ to $D - 1$)	First 3 days of HWs ($D + 0$ to $D + 2$)	All days in HWs	Mean DJF freq. (%)	Days before CSPs ($D - 3$ to $D - 1$)	First 3 days of CSPs ($D + 0$ to $D + 2$)	All days in CSPs
A	13.2	1.6*	0.7	0.6	12.1	0.7	2.5*	1.9*
AN	4.6	1.2	0.2	0.5	2.4	2.7*	0.9	1.9
ANE	3.8	2.2*	0.0*	0.6	2.0	1.7	0.6	1.7
AE	4.4	2.7*	1.5	1.5	2.1	4.0*	2.5	3.1*
ASE	2.7	2.0*	2.4*	2.1*	2.8	0.8	4.7*	3.6*
AS	1.7	1.3	2.6	1.7	3.4	0.3	2.2*	2.4*
ASW	3.5	0.9	2.5*	2.2*	5.7	0.0*	0.6	0.7
AW	5.7	0.4*	1.0	0.6	12.0	0.5*	0.0*	0.2*
ANW	6.6	0.8	0.5	0.3*	5.7	0.6	0.8	0.4
N	3.8	0.6	0.6	0.4*	1.7	3.7*	0.6	0.6
NE	4.8	1.4	0.2	0.3*	1.6	1.4	2.1	1.4
E	4.1	2.1	1.6	1.4	2.9	3.0*	2.2*	3.5*
SE	3.1	0.4	5.2*	4.1*	3.9	1.1	1.7	2.1*
S	2.3	2.3*	0.9	0.9	3.4	0.6	0.0	0.3*
SW	4.2	0.8	1.8	1.5	7.1	0.3*	0.5	0.4*
W	5.6	0.0*	0.4*	0.4*	10.7	0.3*	0.3*	0.2*
NW	4.6	0.2*	0.0*	0.2*	5.4	1.0	0.4	0.3*
CN	1.7	0.6	0.0	0.0	0.7	4.6*	0.0	0.0
CNE	2.1	0.5	0.0	0.3	0.6	8.6*	1.7	0.9
CE	2.7	0.4	0.4	1.1	1.6	0.7	1.4	0.7
CSE	1.7	0.0	3.1*	2.5	1.9	1.7	0.6	1.2
CS	1.3	0.0	3.3*	2.2	2.0	1.1	0.6	0.6
CSW	1.9	0.6	1.2	1.6	2.2	0.0	0.0	0.0*
CW	1.8	0.0	0.6	1.2	2.1	1.0	0.0	0.0*
CNW	1.9	0.6	0.0	0.8	1.4	1.5	0.0	0.0
C	3.2	0.3	0.7	1.1	2.6	3.0*	0.8	0.7
Anticyclonic	46.2	1.4*	1.0	0.9	48.1	0.8	1.4*	1.3*
Cyclonic	18.3	0.4*	0.9	1.1	15.0	1.8*	0.5	0.4*
Southerly	22.4	1.0	2.5*	2.1*	32.4	0.5*	1.1	1.2
Westerly	35.7	0.5*	0.8	0.8	52.3	0.5*	0.3*	0.3*
Northerly	33.9	1.0	0.2*	0.4*	21.5	1.8*	0.7	0.7
Easterly	29.5	1.5*	1.5*	1.4*	19.3	2.0*	2.1*	2.3*

Sum of the supertypes' frequencies exceeds 100 % because of overlaps between the supertypes (see Sect. 2.2.2)

Asterisk (*) indicates values of the efficiency coefficient higher (lower) than the 95 % (5 %) quantile of the estimated seasonal distribution using the Monte Carlo method. Types conducive to HWs or CSPs are highlighted in *bold*

3 Results

3.1 Statistics for heat waves and cold spells in observed data and RCMs

3.1.1 Heat waves

The RCMs tend to simulate higher frequencies of summer HWs compared to the observed data, as shown in Table 3. While there were 31 observed HWs during the examined 30-year period, the mean number of HWs simulated by the RCMs is 35. In four models, the frequency of HWs is more than one-quarter higher than the observed frequency.

Overestimation in the RCMs is even larger for the total number of days in HWs (Table 3). This indicates that hot days (i.e. those days with TX above the 90 % quantile in summer) tend to be grouped into longer sequences in model simulations than in observations. The total number of hot days is by definition equal to 10 % of all summer days, which corresponds to 276 days over the examined 30-year period. In the observed data, however, only half of them (140, Table 3) are grouped into HWs. In the RCMs, on the other hand, the number of hot days that occur within HWs is on average 169 (ranging from 143 to 205 in individual RCMs), which means that around 60 % of all hot days occur during HWs (the highest value is found for CNRM-Aladin and reaches as high as 74 % of all hot days). This implies that climate models tend to simulate longer persistence of hot days in comparison to observed data.

The RCMs' overall tendency to simulate more and longer sequences of hot days is found also for the frequency of HWs lasting 5 days and more (Table 3). While there were only 11 observed HWs at least 5 days long during 1971–2000, the mean number of such HWs is 14 in the RCMs. Also, for most RCMs, these longer HWs comprise a higher percentage of all HWs compared to the observed data. In the case of ICTP-RegCM, for example, HWs lasting at least 5 days constitute 62 % of all HWs, while that proportion is only 35 % in observations (Table 3).

3.1.2 Cold spells

Analogously to HWs, the frequency of CSPs in winter tends to be higher in the RCM simulations than in the observed data, as 11 out of the 13 RCMs overestimate the number of CSPs (Table 3). In the observed data, the grouping of cold days into CSPs is stronger than that of hot days into HWs, which points to a higher persistence of very cold weather episodes in winter. This is generally captured by all RCMs except for CNRM-Aladin, in which an opposite pattern is found. As the case for hot days in HWs, however, the percentage of cold days occurring during CSPs tends to be overestimated in the RCMs: cold days during CSPs comprise 72–80 % of all cold days in winter in most (11) RCMs, while the percentage of cold days occurring during CSPs is 67 % in the observed data. Moreover, the number of long CSPs (lasting at least 5 days) is higher in all RCMs except one (CNRM-Aladin) in comparison to the observed data.

Table 3 Number of summer HWs and winter CSPs, total number of days in HWs or CSPs, and number of HWs or CSPs at least 5 days long in the observed data (OBS) and in RCMs during 1971–2000

	Number of HWs (diff. in %)	Number of days in HWs (diff. in %)	Number of HWs 5+ days long (in %)	Number of CSPs (diff. in %)	Number of days in CSPs (diff. in %)	Number of CSPs 5+ days long (in %)
OBS	31	140	11 (35)	31	181	14 (45)
C4I	40 (+29)	169 (+21)	15 (38)	34 (+10)	206 (+14)	19 (56)
CHMI	35 (+13)	166 (+19)	13 (37)	39 (+26)	201 (+11)	17 (44)
CNRM	42 (+35)	205 (+46)	17 (40)	36 (+16)	178 (−2)	14 (39)
DMI	35 (+13)	163 (+16)	14 (40)	32 (+3)	212 (+17)	20 (63)
EC	39 (+26)	179 (+28)	11 (28)	31 (+0)	196 (+8)	17 (55)
ETHZ	34 (+10)	159 (+14)	12 (35)	37 (+19)	210 (+16)	19 (51)
HC	30 (−3)	157 (+12)	17 (57)	34 (+10)	198 (+9)	19 (56)
ICTP	29 (−6)	168 (+20)	18 (62)	32 (+3)	207 (+14)	18 (56)
KNMI	35 (+13)	177 (+26)	14 (40)	32 (+3)	183 (+1)	17 (53)
METNO	31 (+0)	161 (+15)	14 (45)	38 (+23)	216 (+19)	16 (42)
MPI	40 (+29)	177 (+26)	14 (35)	36 (+16)	200 (+10)	17 (47)
OURANOS	34 (+10)	167 (+19)	15 (44)	31 (+0)	198 (+9)	17 (55)
SMHI	32 (+3)	143 (+2)	13 (41)	37 (+19)	195 (+8)	20 (54)
Ensemble mean	35 (+13)	169 (+20)	14 (42)	35 (+11)	200 (+10)	18 (52)

3.2 Circulation types conducive to heat waves and cold spells

3.2.1 Observed data

Circulation types conducive to HWs and CSPs are evaluated in terms of an efficiency coefficient calculated as the ratio of the relative frequency of a given type before or during HWs or CSPs to its long-term mean seasonal frequency. Efficiency coefficients for all types and supertypes (see Sect. 2.2.2) in the observed data are given in Table 2 for both summer HWs and winter CSPs.

Anticyclonic, easterly and southerly circulation types are found as types conducive to HWs in Central Europe since their frequencies tend to be higher during days preceding the onset of a HW. For the anticyclonic and easterly super-types, as well as the A, AE, ANE, ASE and S types, the efficiency coefficients are significantly >1 (Table 2). During HWs, an increased frequency of types with southerly flow is evident: the frequency of the SE type is 5 times higher

during the first 3 days of HWs than its seasonal mean, and also for the entire southerly supertype the increase is statistically significant. On the other hand, cyclonic, northerly and westerly flows are generally not linked to HWs. While the types conducive to HWs are not surprising per se, the results reveal a clear radiation-to-advection pattern: anticyclonic circulation types with a small cloud amount and dominant positive radiative balance prevail before the onset of a HW, while types in which warm advection plays a more important role become dominant during HWs and support their development and persistence. The radiation-to-advection transition is illustrated also by composites of the mean sea level pressure fields on individual days (from 3 days before a HW to 2 days after a HW's onset, Fig. 4): the patterns correspond to a high pressure area moving from SW to NE across Europe, with warm southerly advection in Central Europe on days $D - 1$ to $D + 1$ while northerly or north-easterly flow occurs on days $D - 3$ and $D - 2$. An influence of a positive radiative balance on days before and during the onset of HWs is supported by

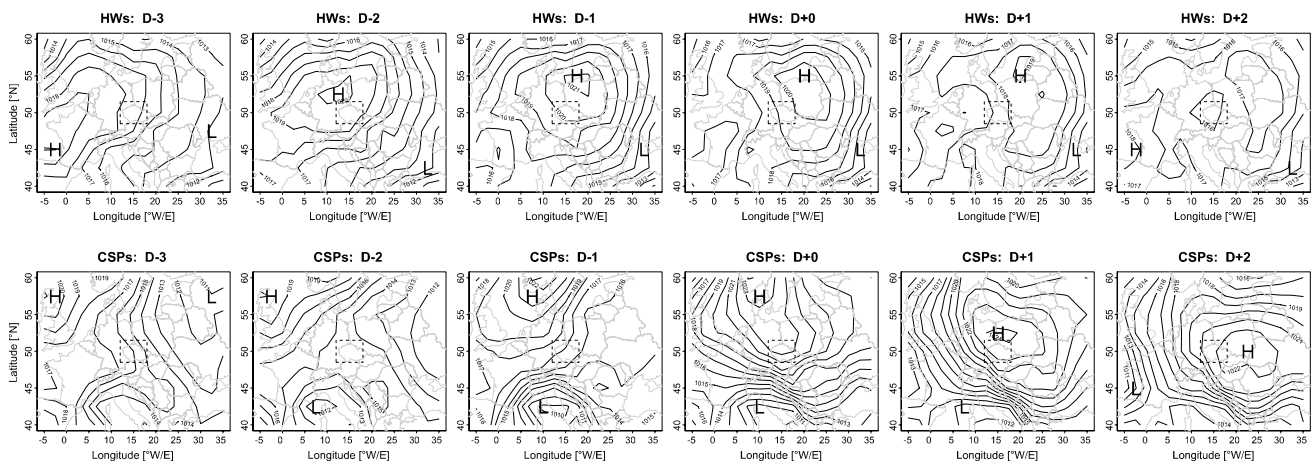
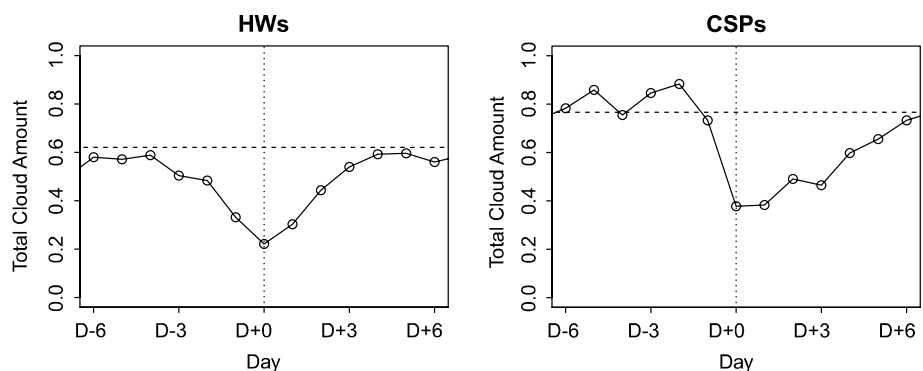


Fig. 4 Mean sea level pressure fields averaged over individual days, from 3 days before ($D - 3$) to 2 days after ($D + 2$) the onset of summer heat waves (winter cold spells). H/L marks areas of high/low

pressure; the dashed line shows the area under study. Data from the ERA-40 reanalysis over 1971–2000 were used

Fig. 5 Mean total cloud amount averaged over individual days from 6 days before ($D - 6$) to 6 days after ($D + 6$) the onset of summer heat waves (winter cold spells). Horizontal line shows the seasonal mean. Data from the Milešovka station were used



the analysis of total cloud amount. Figure 5 shows that the mean cloud cover on days preceding HWs as well as during the first days of HWs is markedly below the seasonal mean.

In winter, the types conducive to CSPs are typically those with easterly and northerly flows, as well as the strongly cyclonic type. For the easterly, cyclonic, and northerly supertypes, the efficiency coefficients are significantly higher on days before the onset of a CSP (Table 2). During the days of CSPs, relative frequencies of anticyclonic types are elevated while there are fewer cyclonic flow days. Westerly types are clearly not conducive to CSPs. In contrast to HWs, an opposite advection-to-radiation effect is found in the observed data for CSPs, with cold (northerly or easterly) advection being more important before the onset of a CSP while radiative cooling during anticyclonic conditions supports the persistence of cold weather (Fig. 4). Figure 5 shows that the days of CSPs are characterized by reduced cloud amount, and there is a sharp drop in cloudiness between days $D - 1$ and $D + 0$. Enhanced frequency of cyclonic types before CSPs (for CN and CNE, the frequency before CSPs is 5–9 times higher compared to the seasonal mean, and the strongly cyclonic type is 3 times more frequent) may also be related to an occurrence of snowfall (cf. Bednorz 2011), and clear-sky anticyclonic conditions during the following days may be particularly favourable for developing very low daily minima of surface air temperature over snow-covered areas.

3.2.2 Model data

As the comparison in Fig. 6 illustrates, although the RCMs are generally able to reproduce the observed circulation types conducive to HWs in summer and CSPs in winter, differences do exist in relation to sampling variability and low frequencies of some circulation types. All RCMs agree with observations that the strongly anticyclonic type is conducive to HWs before their onset, and in one RCM its frequency is elevated also during HWs. All RCMs also simulate enhanced frequencies of at least three types with south advection during HWs (mainly AS, S, SE). A reasonably good reproduction of links to circulation types in the RCMs is found also for CSPs, but the results are slightly more scattered compared to those for HWs (Fig. 6). The frequency of the strongly anticyclonic type is enhanced during CSPs in all RCMs, and anticyclonic and easterly types dominate during CSPs in the RCMs. These results are in line with the observed data. The RCMs also generally capture the fact that northerly and cyclonic types (often associated with heavy snowfall in Central Europe, Bednorz 2011) are conducive to CSPs before their onset.

Due to the low frequency of some circulation types (especially hybrid cyclonic types, see Fig. 2), quantitative comparison is given for supertypes (Fig. 7). All RCMs produce efficiency coefficients greater than 1 (mostly significantly) for the anticyclonic super-type in days preceding HWs, as well as for the southerly super-type during HWs. The frequency of the easterly super-type is elevated

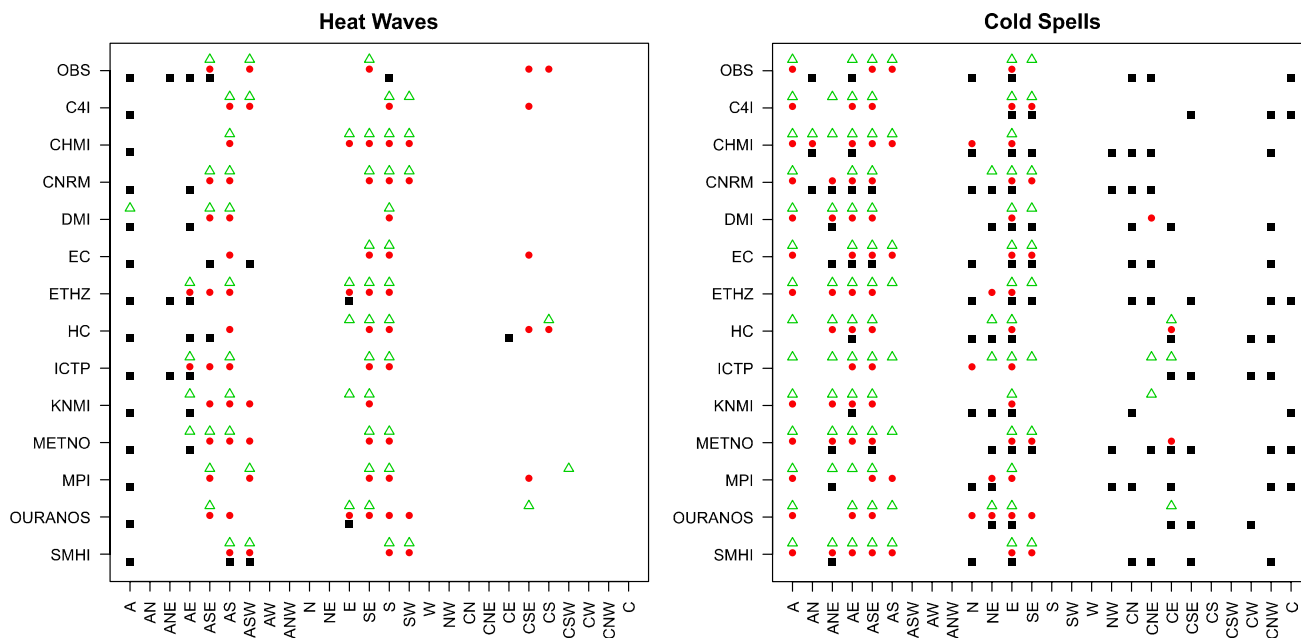


Fig. 6 Circulation types conducive to heat waves and cold spells in the observed data and RCMs: *points* indicate efficiency coefficients significantly >1 (more details on statistical significance are given in

Sect. 2.2.3). *Squares*—for 3 days before the beginning of HWs or CSPs ($D - 3$ to $D - 1$); *circles*—for the first 3 days of HWs or CSPs ($D + 0$ to $D + 2$); *triangles*—for all days of HWs or CSPs

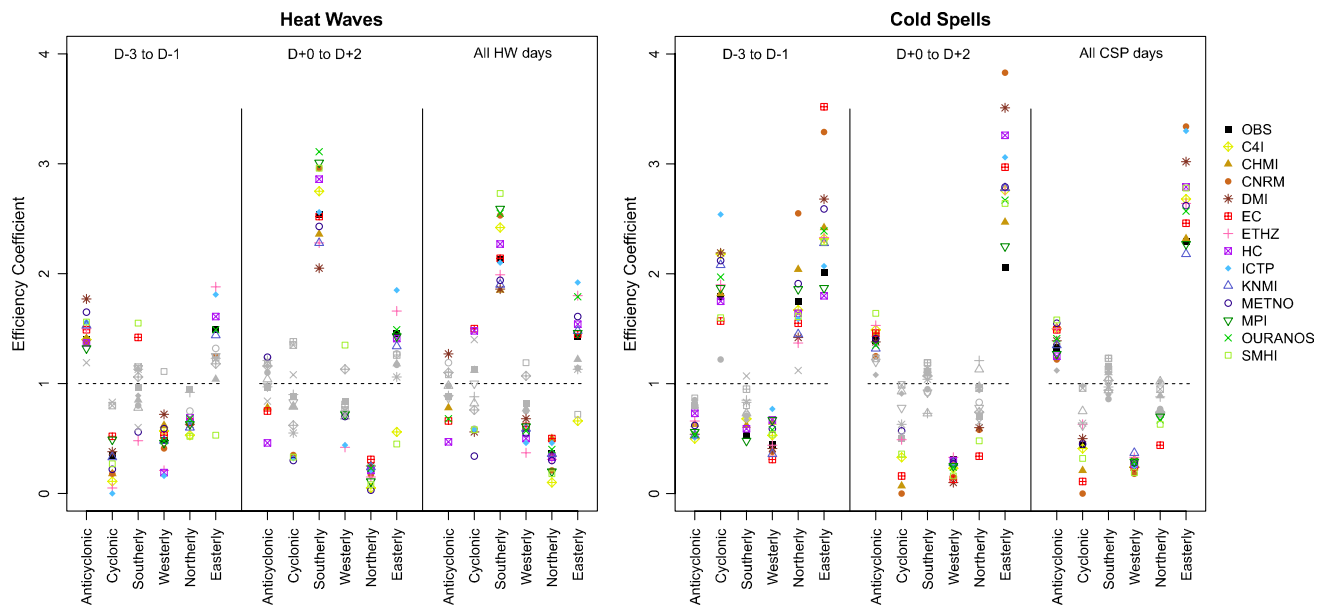


Fig. 7 Efficiency coefficients of supertypes for 3 days before the beginning of HWs or CSPs ($D - 3$ to $D - 1$), the first 3 days of HWs or CSPs ($D + 0$ to $D + 2$), and all days in HWs or CSPs for observed

data and RCM simulations. Values of the efficiency coefficient insignificantly different from 1 are shown in grey (more details on statistical significance are given in Sect. 2.2.3 and Table 2)

in most RCMs both before and during HWs. The observed low frequency of the cyclonic superotype before HWs and of the northerly superotype both before and during HWs is captured by the models, too. With respect to CSPs, all RCMs reproduce a higher frequency of the cyclonic, easterly and northerly superotypes and a lower frequency of the anticyclonic and westerly superotypes before the beginning of CSPs. An elevated frequency of the easterly and anticyclonic superotypes during CSPs is captured by all RCMs as well.

These findings indicate that the RCMs are generally able to reproduce basic features of the observed radiation-to-advection effect of circulation types for HWs and an opposite advection-to-radiation effect for CSPs.

3.3 Links between the persistence of circulation and temperature anomalies

In this section, in order to illustrate how the RCMs capture magnitudes of the anomalies and their temporal patterns, we analyse temperature anomalies on the first 5 days of sequences of individual circulation superotypes while focusing on the superotypes conducive to HWs or CSPs. The length of 5 days is chosen as it represents the longest mean length of sequences of days with a given circulation superotype (westerly in winter) for the ensemble mean (Table 4). Note that the mean length of the sequences is only 2–3 days for most other superotypes, and so the first 5 days of all sequences capture a large majority (89 % on average in the observed data) of days with a given superotype.

The temperature anomaly on the N th day is averaged over all N th days of all sequences of a given superotype at least N days long (i.e. for the first day, also sequences one day long are included). Involving additional days does not change the basic patterns but introduces large variability due to sharply declining sample sizes for the sixth and further days. We remind that anomalies from the mean annual cycle are calculated for each individual RCM separately, and thus they do not reflect temperature bias of a given RCM (Sect. 2.2.1). How the length of a sequence affects mean temperature in the observed and model data is shown in Fig. 8.

In summer, for all three superotypes conducive to HWs—anticyclonic, southerly and easterly (Table 2 and Fig. 7)—temperature increases during sequences of days with the given circulation pattern. The observed increases are relatively well reproduced by the RCMs (Fig. 8). For the anticyclonic superotype, the mean increase between the first and fifth day of a sequence is $3.5\text{ }^{\circ}\text{C}$ in the observed data, and it is $3.1\text{ }^{\circ}\text{C}$ averaged over the RCMs (with range $2.0\text{--}5.3\text{ }^{\circ}\text{C}$). For the southerly superotype, there is an observed increase of $2.3\text{ }^{\circ}\text{C}$ between the first and fourth day, and the average modelled increase is $2.2\text{ }^{\circ}\text{C}$, although the RCMs produce a rather large spread from 0.5 to $4.9\text{ }^{\circ}\text{C}$ [note that the sequences are typically much shorter for the southerly superotype (cf. Table 4), and that contributes to the large sampling variability]. A small gradual increase of temperature anomalies for the easterly superotype is captured by all RCMs. On the other hand, sequences several days in length for the westerly and northerly superotypes (associated with

Table 4 Summer and winter mean lengths of day sequences within given circulation supertypes in the observed data (OBS) and RCMs during 1971–2000

	Anticyclonic	Cyclonic	Southerly	Westerly	Northerly	Easterly
JJA						
OBS	2.58	1.80	1.62	2.74	1.94	3.03
C4I	3.42**	1.86	1.91**	3.24**	2.39**	3.13
CHMI	3.53**	1.83	1.65	3.02*	2.18**	3.99**
CNRM	4.38**	1.79	1.84**	2.45	2.18**	4.04**
DMI	3.20**	1.95	1.93**	3.48**	2.62**	3.45*
EC	3.06**	1.73	1.62	2.70	2.47**	3.60**
ETHZ	2.95**	1.90	1.72*	3.04**	2.72**	3.77**
HC	2.92**	1.86	1.58	2.90	2.23**	3.40
ICTP	3.59**	1.88	1.74	3.68**	2.65**	3.47**
KNMI	3.67**	1.96**	1.80**	2.73	2.62**	4.08**
METNO	3.48**	1.97	1.91**	3.59**	2.49**	3.12
MPI	3.49**	1.95*	1.91**	3.07**	2.57**	3.79**
OURANOS	3.50**	2.01**	1.54	3.82**	2.82**	3.76**
SMHI	3.30**	1.85	1.92**	3.31**	2.51**	3.19
Ensemble mean	3.42	1.89	1.77	3.16	2.50	3.60
DJF						
OBS	3.11	1.67	2.63	4.24	1.71	2.53
C4I	3.41	2.06**	2.95	5.32**	2.21**	2.81*
CHMI	3.78**	1.79**	2.97**	5.73**	1.94**	2.98**
CNRM	4.80**	1.71	3.01**	5.04**	2.05**	2.61
DMI	3.34	2.05**	2.88	4.95*	2.30**	2.72
EC	3.64**	1.91**	2.94**	5.60**	2.07**	2.93**
ETHZ	3.57	2.01**	3.17**	5.06**	2.36**	2.81**
HC	2.96	1.79	2.76	5.41**	2.00**	2.85**
ICTP	3.25	1.99**	2.62	6.11**	2.23**	2.61
KNMI	3.74**	2.07**	3.22**	5.55**	2.17**	3.23**
METNO	3.34	1.89**	3.03**	5.30**	2.21**	2.58
MPI	3.47	1.96**	2.94	5.04**	2.12**	2.85**
OURANOS	3.29	1.70**	2.77	5.85**	2.11**	2.73*
SMHI	3.44	2.00**	2.93	5.49**	2.18**	2.87**
Ensemble mean	3.54	1.92	2.94	5.42	2.15	2.81

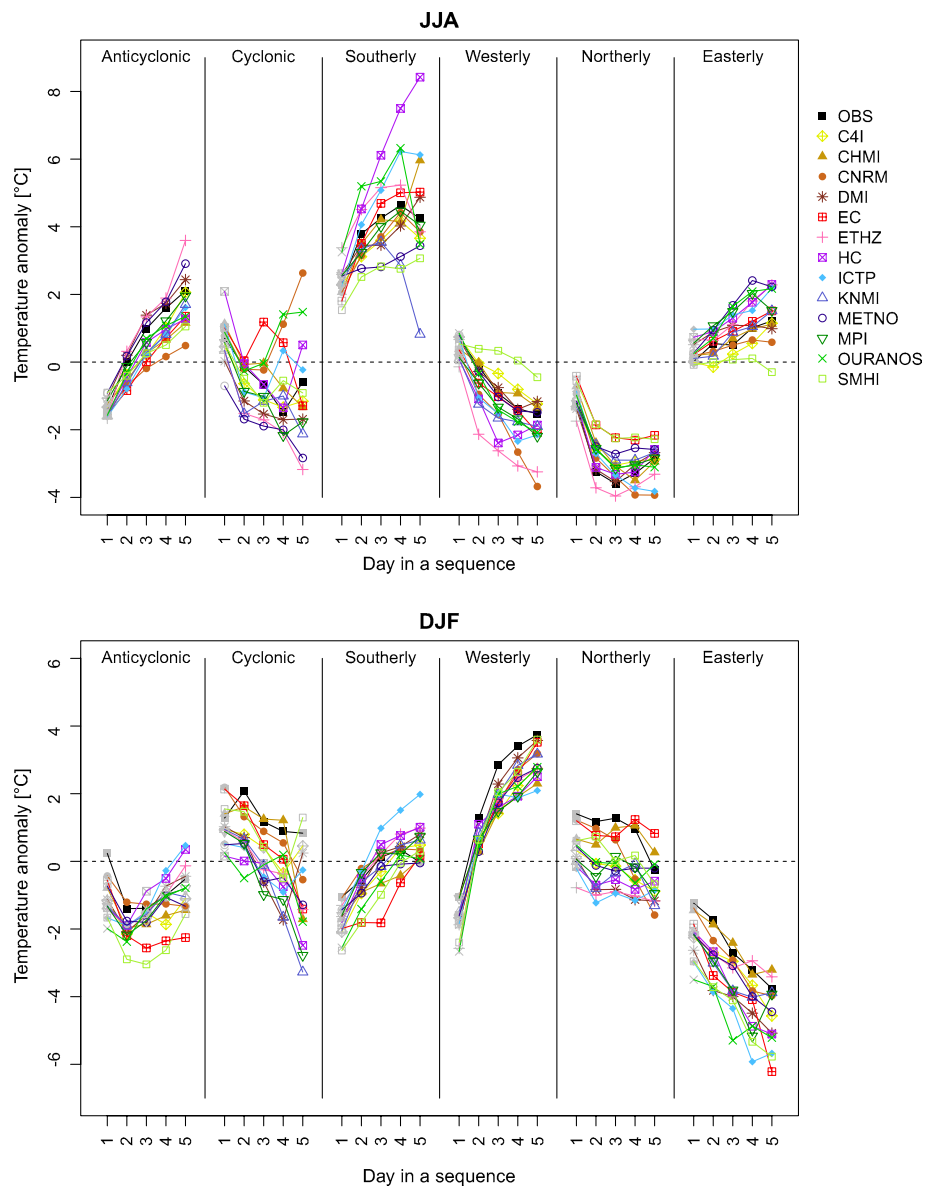
* (**) indicates when sequences are significantly longer in the RCM than in the observed data according to the Wilcoxon–Mann–Whitney test at $p = 0.1$ ($p = 0.05$)

advection of relatively cold maritime air to Central Europe in summer) tend to produce decrease in temperature anomalies, and these are again reproduced by the RCMs. The interdiurnal temperature changes during sequences of days with a given supertype illustrate typical physical mechanisms playing roles in Central Europe: positive radiative balance in case of the anticyclonic type, warm advection for the southerly and easterly types, and cold advection for the westerly and northerly types. The fact that the RCMs capture these day-to-day changes for all the supertypes suggests that the underlying mechanisms are simulated reasonably well.

Similarly in winter, sequences of supertypes leading to CSPs (easterly, cyclonic and northerly; Fig. 4) are linked to a progressive decrease of temperature anomalies (Fig. 8).

Especially days within the easterly supertype are characterized by negative temperature anomalies from the mean annual cycle, and the magnitude of the anomalies tends to increase with the length of the sequences of these days (the mean change during the first 5 days is -2.5 °C in the observed data, and for the RCMs it ranges from -1.3 to -4.6 °C with a mean of -2.4 °C). It may be somewhat surprising that the northerly supertype is associated with neither pronounced negative temperature anomalies nor gradual decline of temperature (which is true for observed data as well as the RCMs). One must take into account that the NW types are associated with advection of a relatively warm maritime air mass in winter (mean observed TN anomaly in days with NW flows is $+2.8$ °C, while it is $-1.6/+0.1$ °C in days with NE/N flows), and they are more

Fig. 8 Mean temperature anomalies on the first 5 days of sequences of days classified within a given circulation super-type in the observed data and RCMs during 1971–2000. Daily maximum temperature in summer and minimum temperature in winter were used. If the mean over the N th day ($N = 2–5$) is insignificantly different from the mean over the first day of the sequences at the 0.05 level, then the point is plotted in grey. The critical values were estimated by bootstrapping [$R = 1000$, the same number as the number of sequences of at least the given length (2–5 days) were resampled from the pool of temperature anomalies during the first N days of sequences]



frequent than the NE and N types (Fig. 2). Figure 8 also shows that the southerly and westerly super-types (which are not linked to CSPs) are characterized by an increase of temperature anomalies. Again, these links reflect mainly differences between colder continental and milder oceanic climates in winter: the advection of cold (warm) air consequently leads to an increase in the magnitude of the negative (positive) temperature anomaly as those conditions persist. As in summer, the RCMs generally reproduce the observed relationships between the persistence of super-types and temperature anomalies in winter.

We conclude that longer sequences of days with circulation patterns conducive to HWs or CSPs support longer duration of HWs or CSPs, since, as shown in Fig. 8, the longer is the sequence the larger tends to be the temperature anomaly. Individual HWs and CSPs are typically

linked to sequences several days long of those types conducive to HWs or CSPs.

3.4 Persistence of circulation types

Since there are strong links between the persistence of circulation types and day-to-day temperature changes, and since these may affect the onset and duration of HWs or CSPs, our focus in this section is on the persistence of atmospheric circulation as simulated by the RCMs. We are primarily interested whether the biases in simulated circulation persistence are related to biases in the characteristics of HWs and CSPs described in Sect. 3.1 (Table 3). The observed and simulated mean lengths of day sequences within given circulation super-types are shown in Table 4.

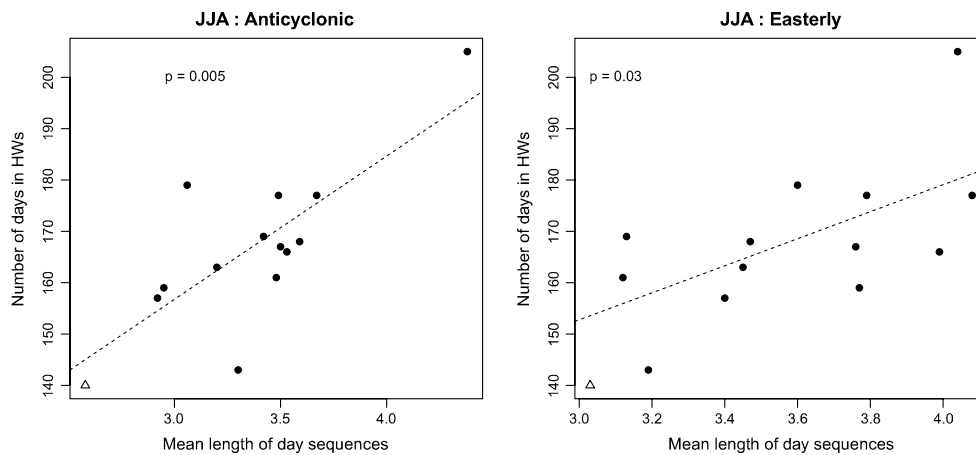


Fig. 9 Scatter plot of mean length of sequences within anticyclonic and easterly circulation supertypes and the number of days in HWs in individual RCMs. *Black points (triangles)* stand for RCMs (*observation*). The level of significance for linear regression over the RCM data is shown

The sequences of days having the same circulation supertype tend generally to be longer in the RCMs than in the observed data. This holds true for both winter and summer, for all circulation supertypes, and for all RCMs examined. There are only very few exceptions in which the mean length of a supertype is shorter in an RCM than in the observed data, mostly in summer (Table 4). In many cases, overestimation of the mean lengths by the RCMs is statistically significant. The tendency towards too-long sequences is greatest for the anticyclonic types in summer (significantly overestimated in all RCMs) and for the westerly types in winter. It is evident from Table 4 that overestimating the persistence of the supertypes conducive to HWs or CSPs is a general feature within the examined ensemble of RCMs. For individual RCMs, we find that with increasing overestimation of the mean length of sequences for anticyclonic and easterly supertypes in summer the number of days in HWs tends to be larger (Fig. 9). Analogous links are insignificant in winter.

Since long sequences of days with circulation patterns conducive to HWs or CSPs support development of longer-lasting HWs or CSPs, the overestimation of the persistence of these supertypes contributes to the overestimated frequency of long HWs and CSPs in the RCMs.

4 Discussion

Anticyclonic and easterly circulation supertypes were detected to be conducive to HWs in summer. Their frequencies are generally greater during days preceding the beginning of a HW, while during HWs an increased frequency of the southerly supertype is evident. This indicates that before the onset of a HW an important role is played by positive radiative balance due to small cloud amount during

anticyclonic situations. In addition to the suppressed cloud cover, these situations are related to precipitation deficit in the affected area. The important role of the precedent precipitation deficit for the development of HWs was shown by Fischer et al. (2007). Using climate model simulations, Jaeger and Seneviratne (2011) demonstrated that extremely high temperatures in summer are strongly affected by the absolute value of soil moisture. A lack of soil moisture results in reduced latent heat flux at the expense of sensible heat flux which brings the additional warming (e.g. Haarsma et al. 2009), and heightens the severity of a HW. Since this soil-moisture feedback is strongest in summer (Stegehuis et al. 2013), apart from a large-scale flow, the severity of HWs also is linked to land–atmosphere feedback (i.e. to internal conditions within the RCMs domain). Warm advection, on the other hand, becomes increasingly important during HWs (Domonkos et al. 2003; Kyselý 2007; Andrade et al. 2012) and even some cyclonic types appear among those with significantly increased frequency during HWs. The importance of persistent anticyclonic conditions over Europe for development of the 2003 heat wave was demonstrated by Black et al. (2004) and Luterbacher et al. (2004), and for the 1992 and 1994 heat waves in Central Europe by Kyselý (2002). The present study, however, reveals that the typical circulation patterns differ before and during HWs, with a clear radiation-to-advection shift occurring over time.

For CSPs in winter, on the other hand, advection plays a more important role before their onset while days within CSPs are typically characterized by negative radiative balance (higher relative frequency of easterly and northerly flows before CSPs vs. higher frequency of anticyclonic types during CSPs). Somewhat surprisingly, cyclonic types are found to have increased frequency on days directly preceding CSPs, and this may also be associated with snowfall

(Bednorz 2011). When followed by anticyclonic conditions, this enhances negative anomalies of daily minimum temperatures through the enhanced albedo of snow-covered surface.

Efthymiadis et al. (2011) found influences of large-scale atmospheric circulation on Mediterranean temperature extremes to be stronger in winter than in summer, and that is supported also by our results, as the percentage of days before and during CSPs having circulation within the supertypes conducive to CSPs in winter is higher than the analogous percentage for HWs in summer (85 vs. 73 %).

Mean temperature anomalies during the sequences of days classified within a given circulation supertype in Fig. 8 show that although the RCMs are able to capture observed magnitudes of the progressive changes of temperature anomalies, they tend to bias the temperature towards colder values during the sequences in winter. This could indicate that the RCMs generally overrate the cooling effect of the continental advection, while they underrate the warming effect of oceanic advection.

Although there are differences among individual models, and especially in the magnitude of the characteristics or links, the main biases in model simulations are similar across most of the RCMs. Some biases in simulation of a meteorological characteristic by an individual model could be explained by the model's performance for other meteorological variables and the links between them. For example, stronger overestimation of the frequency of HWs and the number of long HWs in CNRM-Aladin (Table 3) is likely linked to the higher frequency and persistence of anticyclonic flows (Fig. 2; Table 4) simulated by this RCM (Fig. 9).

We have focused on the ability of climate models to capture large-scale atmospheric circulation because this is important for the reproduction of surface air temperatures (cf. Plavcová and Kyselý 2012). In the present study, we extended the analysis to links between atmospheric circulation (characterized by frequency of types/supertypes and their persistence) and spells of high and low temperature extremes. We showed that current RCMs capture the links between circulation and spells of extreme temperatures relatively well in both seasons. Our results nevertheless point to the importance of biases in the simulated circulation persistence. Overestimation of the persistence was detected to be a general bias of the examined RCMs. This contributes to increased persistence of temperature extremes in the simulated data and hence also to too-frequent and too-long simulated HWs and CSPs. The tendency of climate models to overestimate the persistence of circulation types seems to be a general issue that has been reported in several previous studies (Huth 1997; Casado and Pastor 2012; Rohrer 2012) without offering clear indications as to possible sources of this bias.

Biases similar to those for the recent climate are likely to be manifested in climate model simulations for future decades. Considering that daily atmospheric circulation associated with temperature extremes will probably remain unchanged in future (Cattiaux et al. 2012), scenarios for the frequency and duration of HWs and CSPs need therefore to be interpreted with a view to the limitations and deficiencies found in the models' performance for the present climate.

5 Conclusions

We show that the ERA-40 driven RCMs tend to simulate higher frequencies of summer HWs and winter CSPs compared to observations in Central Europe over the reference period 1971–2000 and that this overestimation is even greater for longer HWs and CSPs. We attempt to explain this bias by analysing persistence of atmospheric circulation conducive to HWs and CSPs in the model simulations.

The RCMs are generally able to reproduce links between circulation and HWs or CSPs. They capture basic features of the observed radiation-to-advection effect for summer HWs: anticyclonic circulation types (with a small cloud amount and dominant positive radiative balance) prevail before the onset of a HW, while types in which warm advection plays a more important role (i.e. those with southerly and easterly flows) become dominant during HWs and support their development and persistence. In winter, the opposite advection-to-radiation effect during CSPs is also reproduced by the RCMs, namely the importance of cold advection before the onset of a CSP and that of radiative cooling during anticyclonic conditions supporting the persistence of cold weather.

Analysis of changes in mean temperature anomalies during sequences of given circulation types reveals a tendency towards gradually increasing temperature during the types conducive to HWs and decreasing temperature during the types conducive to CSPs. These features are captured in the RCMs reasonably well. Since mean lengths of all circulation supertypes are overestimated in the RCMs (mostly significantly), we conclude that the overly persistent circulation in climate models contributes to the overestimated frequency and duration of simulated HWs and CSPs.

As these biases are rather general among the examined RCMs and similar drawbacks are likely to be manifested in climate model simulations for the twenty-first century, the results also suggest that climate change scenarios for spells of days with high or low temperatures need to be interpreted with caution. More effort is needed to understand the causes of the overestimated persistence of circulation patterns in climate models and how these biases may influence other simulated characteristics for which day-to-day

temperature variability is important, such as dry spells and multi-day precipitation events.

Acknowledgments The RCM data were obtained from the ENSEMBLES project database funded within the EU-FP6, contract number 505539. The study was supported by the Czech Science Foundation under project P209/10/2265 and by the Ministry of Education under project 7AMB15AR001. We thank Ondřej Lhotka, Institute of Atmospheric Physics, Prague, for his valuable comments on the draft of the paper, and anonymous referees for suggestions that helped improve the original manuscript.

References

- Alexander LV, Zhang X, Peterson TC et al (2006) Global observed changes in daily climate extremes of temperature and precipitation. *J Geophys Res* 111 Art. No. D05109
- Andrade C, Leite SM, Santos JA (2012) Temperature extremes in Europe: overview of their driving atmospheric patterns. *Nat Hazards Earth Sys* 12(5):1671–1691
- Ballester J, Rodó X, Giorgi F (2010) Future changes in Central Europe heat waves expected to mostly follow summer mean warming. *Clim Dyn* 35:1191–1205. doi:10.1007/s00382-009-0641-5
- Barriopedro D, Fischer EM, Luterbacher J, Trigo RM, García-Herrera R (2011) The hot summer of 2010: redrawing the temperature record map of Europe. *Science* 332:220–224. doi:10.1126/science.1201224
- Bednorz E (2011) Synoptic conditions of the occurrence of snow cover in central European lowlands. *Int J Climatol* 31(8):1108–1118
- Beniston M (2004) The 2003 heat wave in Europe: a shape of things to come? An analysis based on Swiss climatological data and model simulations. *Geophys Res Lett* 31:L02202. doi:10.1029/2003GL018857
- Beniston M, Stephenson DB, Christensen OB, Ferro CAT, Frei C, Goyette S, Halsnaes K, Holt T, Jylhä K, Koffi B, Palutikof J, Schöll R, Semmler T, Woth K (2007) Future extreme events in European climate: an exploration of regional climate model projections. *Clim Change* 81:71–95. doi:10.1007/s10584-006-9226-z
- Black E, Blackburn M, Harrison G, Hoskins B, Methven J (2004) Factors contributing to the summer 2003 European heatwave. *Weather* 59:217–223. doi:10.1256/wea.74.04
- Blenkinsop S, Jones PD, Dorling SR, Osborn TJ (2009) Observed and modelled influence of atmospheric circulation on central England temperature extremes. *Int J Climatol* 29:1642–1660
- Böhm U, Kücken M, Ahrens W, Block A, Hauffe D, Keuler K, Rockel B, Will A (2006) CLM—the climate version of LM: brief description and long-term application. *COSMO Newsl* 6:225–235
- Casado MJ, Pastor MA (2012) Use of variability modes to evaluate AR4 climate models over the Euro-Atlantic region. *Clim Dyn* 38(1–2):225–237
- Cassou C, Terray L, Phillips AS (2005) Tropical Atlantic influence on European heat waves. *J Clim* 18:2805–2811
- Cattiaux J, Yiou P, Vautard R (2012) Dynamics of future seasonal temperature trends and extremes in Europe: a multi-model analysis from CMIP3. *Clim Dyn* 38(9–10):1949–1964
- Christensen JH, Christensen OB, Lopez P, van Meijgaard E, Botzet M (1996) The HIRHAM4 regional atmospheric climate model. Danish Meteorological Institute, Copenhagen, Scientific Report 96–4
- Ciais P, Reichstein M, Viovy N et al (2005) Europe-wide reduction in primary productivity caused by the heat and drought in 2003. *Nature* 437:529–533
- Collins M, Booth BBB, Harris GR, Murphy JM, Sexton DMH, Webb MJ (2006) Towards quantifying uncertainty in transient climate change. *Clim Dyn* 27:127–147
- De Bono A, Giuliani G, Kluser S, Peduzzi P (2004) Impacts of summer 2003 heat wave in Europe. *UNEP/DEWA/GRID Eur Environ Alert Bull* 2:1–4
- Della-Marta PM, Luterbacher J, von Weissenfluh H, Xoplaki E, Brunet M, Wanner H (2007) Summer heat waves over western Europe 1880–2003, their relationship to large-scale forcings and predictability. *Clim Dyn* 29(2–3):251–275
- Demuzere M, Werner M, van Lipzig NPM, Roeckner E (2009) An analysis of present and future ECHAM5 pressure fields using a classification of circulation patterns. *Int J Climatol* 29:1796–1810
- Domonkos P, Kysely J, Piotrowicz K, Petrovic P, Likso T (2003) Variability of extreme temperature events in south-central Europe during the twentieth century and its relationship with large scale circulation. *Int J Climatol* 23:987–1010
- Efthymiadis D, Goodess CM, Jones PD (2011) Trends in Mediterranean gridded temperature extremes and large-scale circulation influences. *Nat Hazards Earth Sys* 11(8):2199–2214
- Farda A, Déqué M, Somot S, Horányi A, Spiridonov V, Tóth H (2010) Model ALADIN as regional climate model for Central and Eastern Europe. *Stud Geophys Geod* 54(2):313–332
- Fischer EM, Schär C (2010) Consistent geographical patterns of changes in high-impact European heatwaves. *Nat Geosci* 3:398–403. doi:10.1038/ngeo866
- Fischer EM, Seneviratne SI, Lüthi D, Schär C (2007) Contribution of land-atmosphere coupling to recent European summer heat waves. *Geophys Res Lett* 34:L06707. doi:10.1029/2006GL029068
- Francis JA, Vavrus SJ (2012) Evidence linking Arctic amplification to extreme weather in mid-latitudes. *Geophys Res Lett* 39:L06801. doi:10.1029/2012GL051000
- Giorgi F, Bi X, Pal JS (2004) Mean, interannual variability and trends in a regional climate change experiment over Europe. I. Present-day climate (1961–1990). *Clim Dyn* 22:733–756
- Haarsma RJ, Selten F, Vd Hurk B et al (2009) Drier Mediterranean soils due to greenhouse warming bring easterly winds over summertime central Europe. *Geophys Res Lett* 36:L04705. doi:10.1029/2008GL036617
- Hartmann DL, Klein Tank AMG, Rusticucci M et al. (2013) Observations: atmosphere and surface. In: *Climate change 2013: the physical science basis. Contribution of Working Group I to the Fifth Assessment Report of the Intergovernmental Panel on Climate Change*, Cambridge University Press, Cambridge and New York
- Haugen JE, Haakenstad H (2006) Validation of HIRHAM version 2 with 50 and 25 km resolution. *RegClim General Technical Report No. 9*. pp 159–173
- Haylock MR, Hofstra N, Klein Tank AMG, Klok EJ, Jones PD, New M (2008) A European daily high-resolution gridded data set of surface temperature and precipitation for 1950–2006. *J Geophys Res* 113:D20119. doi:10.1029/2008JD010201
- Huth R (1997) Continental-scale circulation in the UKHI GCM. *J Clim* 10:1545–1561
- Huth R, Kysely J, Bochníček J, Hejda P (2008) Solar activity affects the occurrence of synoptic types over Europe. *Ann Geophys* 26:1999–2004
- Jacob D (2001) A note to the simulation of the annual and interannual variability of the water budget over the Baltic Sea drainage basin. *Meteorol Atmos Phys* 77:61–73

- Jaeger EB, Seneviratne SI (2011) Impact of soil moisture-atmosphere coupling on European climate extremes and trends in a regional climate model. *Clim Dyn* 36(9–10):1919–1939
- Jenkinson AF, Collison FP (1977) An initial climatology of gales over the North Sea. Meteorological Office, Bracknell, Synoptic Climatology Branch Memorandum No. 62
- Jones PD, Hulme M, Briffa KR (1993) A comparison of Lamb circulation types with an objective classification scheme. *Int J Climatol* 13:655–663
- Kirtman B, Power SB, Adedoyin JA et al (2013) Near-term Climate Change: projections and predictability. In: *Climate change 2013: the physical science basis. Contribution of Working Group I to the fifth assessment report of the intergovernmental panel on climate change*, Cambridge University Press, Cambridge and New York
- Kjellström E, Bärring L, Gollvik S, Hansson U et al (2005) A 140-year simulation of European climate with the new version of the Rossby Centre regional atmospheric climate model (RCA3). *SMHI Rep Meteorol Climatol* 108, SMHI, Norrköping, Sweden, p 54
- Kodra E, Steinhäuser K, Ganguly AR (2011) Persisting cold extremes under twenty-first-century warming scenarios. *Geophys Res Lett* 38:1–6. doi:10.1029/2011GL047103
- Kyselý J (2002) Temporal fluctuations in heat waves at Prague–Klementinum, the Czech Republic, from 1901 to 1997, and their relationships to atmospheric circulation. *Int J Climatol* 22:33–50
- Kyselý J (2007) Implications of enhanced persistence of atmospheric circulation for the occurrence and severity of temperature extremes. *Int J Climatol* 27:689–695
- Kyselý J (2008) Influence of the persistence of circulation patterns on warm and cold temperature anomalies in Europe: analysis over the twentieth century. *Glob Planet Change* 62:147–163. doi:10.1016/j.gloplacha.2008.01.003
- Kyselý J (2010) Recent severe heat waves in central Europe: how to view them in a long-term prospect? *Int J Climatol* 109:89–109. doi:10.1002/joc1874
- Kyselý J, Huth R (2006) Changes in atmospheric circulation over Europe detected by objective and subjective methods. *Theor Appl Climatol* 85:19–36
- Kyselý J, Plavcová E, Davidkiovová H, Kynčl J (2011) Comparison of hot and cold spell effects on cardiovascular mortality in individual population groups in the Czech Republic. *Clim Res* 49:113–129. doi:10.3354/cr01014
- Lockwood M, Harrison RG, Woollings T, Solanki SK (2010) Are cold winters in Europe associated with low solar activity? *Environ Res Lett* 5:024001. doi:10.1088/1748-9326/5/2/024001
- Luterbacher J, Dietrich D, Xoplaki E, Grosjean M, Wanner H (2004) European seasonal and annual temperature variability, trends, and extremes since 1500. *Science* 303:1499–1503
- Meehl GA, Tebaldi C (2004) More intense, more frequent, and longer lasting heat waves in the twenty-first century. *Science* 305:994–997. doi:10.1126/science.1098704
- Miralles DG, Teuling AJ, Van Heerwaarden CC, De Arellano JV-G (2014) Mega-heatwave temperatures due to combined soil desiccation and atmospheric heat accumulation. *Nat Geosci* 7(5):345–349
- Moberg A, Jones PD, Lister D et al (2006) Indices for daily temperature and precipitation extremes in Europe analyzed for the period 1901–2000. *J Geophys Res* 111:D22106. doi:10.1029/2006JD007103
- Peings Y, Cattiaux J, Douville H (2013) Evaluation and response of winter cold spells over Western Europe in CMIP5 models. *Clim Dyn* 41:3025–3037
- Plavcová E, Kyselý J (2012) Atmospheric circulation in regional climate models over Central Europe: links to surface air temperature and the influence of driving data. *Clim Dyn* 39:1681–1695
- Plavcová E, Kyselý J, Štěpánek P (2014) Links between circulation types and precipitation in Central Europe in the observed data and regional climate model simulations. *Int J Climatol* 34:2885–2898
- Plummer D, Caya D, Côté H, Frigon A, Biner S, Giguère M, Paquin D, Harvey R, de Elia R (2006) Climate and climate change over North America as simulated by the Canadian regional climate model. *J Climate* 19:3112–3132
- Radu R, Déqué M, Somot S (2008) Spectral nudging in a spectral regional climate model. *Tellus* 60A:898–910
- Robine J-M, Cheung SLK, Le Roy S, Van Oyen H, Griffith C, Michel J-P, Herrmann FR (2008) Death toll exceeded 70,000 in Europe during the summer of 2003. *C R Biol* 331:171–178. doi:10.1016/j.crvi.2007.12.001
- Rohrer M (2012) Climate change and circulation types in the Alpine Region. *Scientific Report MeteoSwiss* No. 91
- Samuelsson P, Jones CG, Willen U, Ullerstig A, Gollvik S, Hansson U, Jansson C, Kjellström E, Nikulin G, Wyser K (2011) The Rossby Centre Regional climate model RCA3: mode description and performance. *Tellus* 63A:4–23
- Schneider A, Schubert S, Vargin P et al (2012) Large-scale flow and the long-lasting blocking high over Russia: summer 2010. *Mon Weather Rev* 140:2967–2981. doi:10.1175/MWR-D-11-00249.1
- Sillmann J, Croci-Maspoli M, Kallache M, Katz RW (2011) Extreme cold winter temperatures in Europe under the influence of North Atlantic atmospheric blocking. *J Clim* 24:5899–5913. doi:10.1175/2011JCLI4075.1
- Stegehuis AI, Vautard R, Ciais P et al (2013) Summer temperatures in Europe and land heat fluxes in observation-based data and regional climate model simulations. *Clim Dyn* 41:455–477. doi:10.1007/s00382-012-1559-x
- Tang Q, Zhang X, Yang X, Francis JA (2013) Cold winter extremes in northern continents linked to Arctic sea ice loss. *Environ Res Lett* 8:014036. doi:10.1088/1748-9326/8/1/014036
- Uppala SM, Kallberg PW, Simmons AJ, Andrae U et al (2005) The ERA-40 re-analysis. *Q J R Meteorol Soc* 131:2961–3012
- van der Linden P, Mitchell JFB (eds) (2009) ENSEMBLES: climate change and its impacts: summary of research and results from the ENSEMBLES project. Met Office Hadley Centre, FitzRoy Road, Exeter EX1 3PB, UK
- van Meijgaard E, van Ulft LH, van de Berg WJ, Bosveld FC, van den Hurk BJM, Lenderink G, Siebesma AP (2008) The KNMI regional atmospheric climate model RACMO, version 2.1. KNMI Tech Rep 302. KNMI, De Bilt
- Vautard R, Gobiet A, Jacob D et al (2013) The simulation of European heat waves from an ensemble of regional climate models within the EURO-CORDEX project. *Clim Dyn* 41:2555–2575. doi:10.1007/s00382-013-1714-z
- Vavrus S, Walsh JE, Chapman WL, Portis D (2006) The behavior of extreme cold air outbreaks under greenhouse warming. *Int J Climatol* 26:1133–1147